Combined Breast Microwave Imaging and Diagnosis System

B. L. Oliveira[1], **A. Shahzad**[1], **M. O'Halloran**[1],
R. C. Conceicao[2, 3], **M. Glavin**[1], **and E. Jones**[1]

[1]Electrical and Electronic Engineering, National University of Ireland Galway, Ireland
[2]Institute of Biomedical Engineering, University Oxford, United Kingdom
[3]Instituto de Biofsica e Engenharia Biomdica, FCUL, Portugal

Abstract— This paper presents results from the development and evaluation of a dedicated Computer-Aided Detection and Diagnosis (CAD) system for Microwave Imaging (MWI) of the breast. CAD systems play a very important role in aiding breast cancer detection, since they help minimising the number of false positives usually associated with most breast imaging techniques. Both imaging and diagnosis of the breast are integrated in the proposed system, by using state of the art Microwave Tomography techniques and refined tumour-grading algorithms. With the proposed system, microwave images allow for the isolation of the tumour response in the recorded signals which ultimately leads to improved performances when diagnosing tumours based on their level of malignancy.

1. INTRODUCTION

Several Computer-Aided Detection and Diagnosis (CAD) systems have been proposed in recent years for various breast imaging modalities, such as X-Ray Mammography, which generally involve pre-processing and segmentation of images followed by diagnosis [1]. In the context of breast Microwave Imaging (MWI), the development of a dedicated CAD system combining features both from microwave images and radar return signals with richer information would greatly contribute to the performance of the technique in terms of specificity. In this paper, the authors focus on an improved method for automated diagnosis of breast cancer based on recorded backscattered signals.

MWI is based on the contrast between the dielectric properties of different types of breast tissue at microwave frequencies. The majority of existing studies which considered MWI of the breast have focused primarily on tumour detection, with automated tumour diagnosis usually seen as a secondary concern. Some studies have investigated the use of Radar Target Signatures (RTS) for the classification of tumours [2–5]. The shape, size and, most importantly, the degree of spiculation at the border of a tumour can significantly influence its RTS, thus allowing for the identification of tumours based on their level of malignancy. However, it is unclear whether the performance of these algorithms can provide sufficient information in anatomical and dielectrical heterogeneous scenarios. More recently, different studies have proposed the use of contrast agents to account for dielectric heterogeneity [6, 7]; nevertheless, doubts still remain about the available dielectric contrast from contrast agents and the targeted delivery of these agents to cancerous tissues. Despite all of these challenges, there is a growing demand for dedicated tumour diagnosis algorithms within the MWI community, given their very significant clinical potential. In fact, recent studies have already analysed classification techniques for pre-clinical microwave imaging prototypes, e.g., [8, 9].

In this paper, a new approach for the grading of tumours is proposed, which integrates microwave imaging and diagnosis of breast cancer in a single system. By using well-documented Microwave Tomography (MT) algorithms to reconstruct the dielectric profile of the breast, tumours can be detected and their location within the breast identified with precision. This information can then be used to process the backscattered signals, by accurately extracting the RTS of any tumour detected in the microwave images, while eliminating most of the unwanted existing clutter sources in the signals. The tumour-grading algorithm can then be more efficiently applied to the tumour responses, and provide a more accurate diagnosis of the tumours level of malignancy. The proposed combined breast microwave imaging and diagnosis system is benchmarked against previous studies which examined standard unprocessed microwave signals, by simulating anatomically-accurate Finite Difference Time Domain (FDTD) breast and tumour models.

The remainder of this paper is organised as follows: Section 2 describes the numerical models, simulation setup, the microwave tomography approach, the windowing technique and the tumour diagnosis approach. Evaluation and results obtained with the proposed system are discussed in Section 3. Finally, some concluding remarks are made in Section 4.

2. COMBINED BREAST MICROWAVE IMAGING AND DIAGNOSIS SYSTEM

The framework of the system proposed in this paper is summarised in Figure 1. To summarise the operation of the system, by way of example, a Class 1 breast model from the UWCEM repository [10] containing a tumour labelled as malignant in the upper-outer quadrant is shown. The model is simulated with FDTD, and the resultant signals are used as input to the MT algorithm to reconstruct an image of the breast. This image is then used to identify the location and extent of the tumour, which further allows windowing the tumour response from the original backscattered signals (the tumour response highlighted in red). Finally, the tumour response is diagnosed according to its level of malignancy. The proposed system is benchmarked against previous studies which analysed standard unprocessed backscattered signals for the diagnosis of breast malignancies. Each element of the system will be described in greater detail in the following subsections.

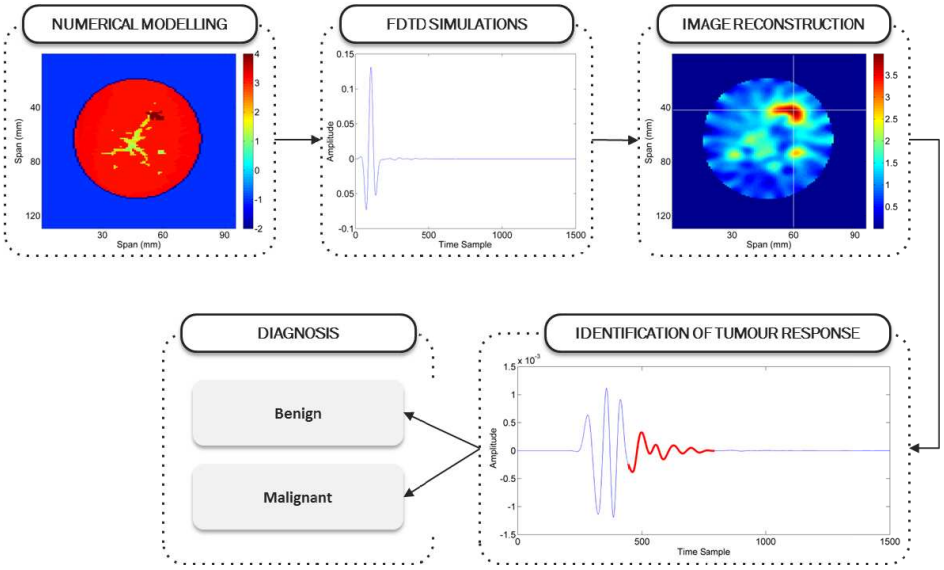

Figure 1: Flowchart of the proposed combined breast microwave imaging and diagnosis system.

2.1. Numerical Modelling and Electromagnetic Simulation

In order to verify the proposed system for the imaging and diagnosis of breast cancer, homogeneous and class 1 numerical breast phantoms adapted from the UWCEM repository [10] were used, where the dielectric properties of different tissue types in the numerical models were derived from the study of Lazebnik et al. [11]. Tumour models of varying sizes and degrees of spiculation were created using the clinically-informed tumour modelling algorithm described in [12]. The tumours were generated with (x, y) diameters of (6, 8), (6, 12), (10, 12), (15, 16) and (18, 10) mm. A degree of spiculation of 0.08 was chosen to generate tumour models with circumscribed margins, which were labelled as benign. For malignant tumours with spiculated and irregular margins, a larger value for of 0.8 was chosen for the degree of spiculation.

The electromagnetic (EM) measurements system was modelled using two concentric rings of Hertzian dipole antennas (each containing 16 antennas) positioned around the breast. The antennas were immersed in a matching medium with dielectric properties equivalent to the fatty tissue, and a differentiated Gaussian pulse with centre frequency of 6 GHz and a -3 dB bandwidth of 6 GHz was used to illuminate the breast model.

2.2. Image Reconstruction and Tumour Windowing

A gradient based time-domain MT algorithm [13] was used to reconstruct the dielectric properties of the breast. In this MT algorithm, the error between measured EM signals from the target object and the computed EM signals from an estimated numerical model of the target is minimized. The least square solution to the minimization problem can be expanded as:

$$F(\epsilon_r, \sigma) = \int_0^T \sum_{m=1}^{M} \sum_{n=1}^{N} W(t) \left| E_{m,n}^{meas}(t) - E_{m,n}^{est}(\epsilon_r, \sigma, t) \right|^2 dt \quad (1)$$

where $E^{meas}_{m,n}(t)$ and $E^{est}_{m,n}(\epsilon_r, \sigma, t)$ are the measured and estimated electrical signals at receiving antenna n corresponding to a transmitted pulse from transmitting antenna m. The weighting factor $W(t)$ is a non-negative weighting function that dictates the behaviour of error functional, and T is the measurement time; M and N are the numbers of the transmitting and receiving points, respectively. The Frchet derivative of the functional $F(\epsilon_r, \sigma)$ is used to derive gradients with respect to relative permittivity, ϵ_r, and conductivity, σ, at each spatial position, $r = (x, y)$ in the reconstruction region.

$$G_{e_r}(r) = 2w_{e_r} \int_0^T \sum_{m=1}^{M} E^{adj}_{m,r}(\epsilon_r, \sigma, t).\frac{d}{dt} E^{est}_{m,r}(\epsilon_r, \sigma, t)dt \tag{2}$$

$$G_{\sigma(r)} = 2w_{\sigma} \int_0^T \sum_{m=1}^{M} E^{adj}_{m,r}(\epsilon_r, \sigma, t)\, E^{est}_{m,r}(\epsilon_r, \sigma, t)dt \tag{3}$$

where $E^{est}_{m,r}(\epsilon_r, \sigma, t)$ is the computed EM field at position r in the reconstruction space due to transmitter m on an estimated model with relative permittivity ϵr, and conductivity σ. The signal $E^{adj}_{m,r}(\epsilon_r, \sigma, t)$ is the solution to Maxwell's adjoint field equations, numerically calculated by reverse time propagation of the difference of measured and estimated EM signals. Additional scaling factors, w_{e_r} and w_{σ} are used to compensate for the variations in sensitivity of the dielectric parameters. The gradients $G_{e_r}(r)$ and $G_{\sigma(r)}$ are in the conjugate gradient method to find the conjugate direction, and the optimal step size α is determined by a line search in the conjugate direction. The dielectric parameters in the kth iteration are updated at each spatial position r in the estimated model according to Equations (4) and (5):

$$\epsilon_r^{k+1} = \epsilon_r^k + \alpha^k d_{\epsilon}^k(r) \tag{4}$$

$$\sigma_r^{k+1} = \sigma_r^k + \alpha^k d_{\sigma}^k(r) \tag{5}$$

where the conjugate directions $d_{\epsilon}^k(r)$ and d_{σ}^k are determined using the Polak-Ribire (PR) method. It is assumed that the skin information is *a priori* known, which is used as an initial estimate in the reconstruction algorithm for realistic class 1 numerical phantoms. Considering the known dielectric properties of tumours, the reconstructed permittivity and conductivity maps are then thresholded to identify the tumour extent and location. Assuming that the average dielectric properties of the breast tissues are available, a time-gating technique is applied to extract the RTS of the tumour based on the round-trip distance between each antenna and the detected tumour. The estimated tumour signature is windowed from the backscattered signal, where the approximate window length is decided empirically by evaluating different window lengths over a dataset of numerical breast phantoms. It is found that a window length of twice the pulse width is appropriate to extract the tumour response from the radar signals. The windowed signals are further used for classification of benign and malignant tumours.

2.3. Tumour Diagnosis

The final step in the proposed system is diagnosing tumours found in the breast according to their level of malignancy. Previous studies have shown promising results by combining feature extraction techniques, namely Principal Component Analysis (PCA), with Support Vector Machines for the classification of tumours in simplified anatomical and dielectric scenarios [4, 5].

PCA is a useful tool which aids in reducing the dimensionality of a dataset. PCA transforms the basis of the original dataset into a new orthonormal basis, allowing the principal components, i.e., the features of the new dataset, to express maximised variance. Here, the variance along each principal component provides a measurement of the relative importance of each dimension. Further details on PCA can be found in [14].

Once the dimensionality of the recorded radar signals is reduced, SVM classifiers can then more efficiently be applied. SVM classifiers use a method to handle nonlinear relations between the input vectors and their corresponding labels by transforming linearly inseparable data to a higher-dimensional space in which they can be more readily separated into the two pre-defined classes of this study: benign or malignant. The system proposed in this paper uses the Radial Basis Function (RBF) kernel to map the tumour data. The kernel parameters are optimised via 10-fold cross-validation, so the best classifier performance can be achieved [15].

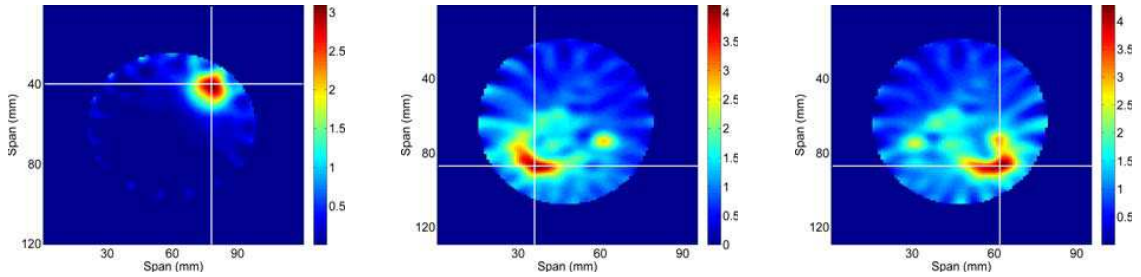

Figure 2: Reconstructed conductivity maps after one iteration of the MT algorithm. (a) Refers to a homogeneous breast with a benign tumour in the upper-inner quadrant; (b) and (c) feature a class 1 breast with a malignant tumour located in the lower-outer quadrant and lower-inner quadrant, respectively.

Table 1: Results of the tumour diagnosis process. Accuracy, sensitivty and specificity are detailed for the homogeneous and class 1 breast types used in this study, for standard unwindowed signals and signals processed with the proposed system.

		Accuracy (%)	Sensitivity (%)	Specificity (%)
Homogeneous Breast	No post-processing	71.6	81.2	61.9
	Proposed system	83.4	95.9	70.9
Class I Breast	No post-processing	63.6	75.3	51.9
	Proposed system	69.5	73.7	65.3

3. RESULTS OF TUMOUR DIAGNOSIS

In Figure 2, results of the MT reconstruction process are shown for the simulated homogeneous and class 1 breast types. For the current implementation of the MT algorithm described in Section 2.2, the authors found that the reconstructed conductivity map yielded a better detection of the extent and location of the tumour, which can be identified by the cross-section of the white lines in Figure 2. For the sake of computational complexity, the tumour extent and location can be identified after a single iteration of the MT algorithm, which is sufficient for the purpose of this study.

As previously mentioned, the diagnosis was performed separately for the homogeneous and class 1 breast types, and included tumours of different sizes and levels of malignancy, placed in different locations within the breast; this diversity in the dataset adds to the complexity of the classification problem. Table 1 details the results of this diagnosis process. For the homogeneous breast type, an improvement of 11.8% in the accuracy of the diagnosis is observed when the proposed windowing of signals is performed; the sensitivity and specificity also improve, by 14.7% and 9%, respectively. For the class 1 breast type, the diagnosis improves by a lower margin of 5.9% when the proposed system is applied. Interestingly, the sensitivity of the diagnosis decreases marginally, but the specificity improves 13.4%. The improvement of the specificity when diagnosing breast tumours is very significant as it ultimately contributes to minimising the false positive rate of MWI as a breast cancer detection technique.

4. CONCLUSIONS AND FUTURE WORK

In this paper, a novel combined breast microwave imaging and diagnosis system has been presented. With this system, images of the breast are generated with MT, and the information obtained from these images is used to produce an automated diagnosis of any tumours found in the breast. The tumour responses are identified and windowed from the recorded signals, and further diagnosed with a refined tumour-grading algorithm. The proposed system was compared to a benchmark system based on standard approaches, where no windowing of tumour responses is performed.

When the system proposed in this paper is applied, the authors observed an improvement in the accuracy of the diagnosis of 11.8% and 5.9% for the homogeneous and class 1 breast types, respectively. Importantly, the specificity of the diagnosis process also improved by 9% and 13.4% for both breast types, which results in less false positive cancers being diagnosed. These results are very significant as they demonstrate the potential of the proposed method to more accurately classify breast tumours according to their level of malignancy in high-clutter scenarios. The clinical applications of a dedicated CAD system for MWI are vast, as there is great interest in finding new

methods that can help minimise the number of false positives usually associated with current breast cancer screening techniques. Future work in this project includes a more detailed analysis of the relationship between the number of PCA components and the accuracy of the SVM classifier. In addition, a study into which pairs of antennas carry more information about the tumour response can impact the performance of the diagnosis process.

ACKNOWLEDGMENT

This work is supported by Science Foundation Ireland (Grants 12/IP/1523 and 1l/SIRG/I2120), EPSRC (EP/J007293/1) and FP7 (MC-IEF-301269) and developed in the framework of COST Action TD1301 (MiMed).

REFERENCES

1. Tang, J., R. M. Rangayyan, J. Xu, T. El Naqa, and Y. Yang, "Computer-aided detection and diagnosis of breast cancer with mammography: Recent advances," *IEEE Trans. Inf. Technol. Biomed.*, Vol. 13, No. 2, 236–251, 2009.
2. Davis, S. K., B. D. Van Veen, S. C. Hagness, and F. Kelcz, "Breast tumor characterization based on ultrawideband microwave backscatter," *IEEE Trans. Biomed. Eng.*, Vol. 55, No. 1, 23–46, 2008.
3. Chen, Y., E. Gunawan, K. S. Low, S.-C. Wang, C.-B. Soh, and T. C. Putti, "Effect of lesion morphology on microwave signature in 2-D ultra-wideband breast imaging," *IEEE Trans. Biomed. Eng.*, Vol. 55, No. 8, 2011–2021, 2008.
4. Conceicao, R. C., M. O'Halloran, E. Jones, and M. Glavin, "Investigation of classifiers for early-stage breast cancer based on radar target signatures," *Progress In Electromagnetics Research* Vol. 105, 295–311, 2010.
5. O'Halloran, M., B. McGinley, R. C. Conceicao, F. Morgan, E. Jones, and M. Glavin, "Spiking neural networks for breast cancer classification in a dielectrically heterogeneous breast," *Progress In Electromagnetics Research*, Vol. 113, 413–428, 2011.
6. Chen, Y., I. J. Craddock, and P. Kosmas, "Feasibility study of lesion classification via contrast-agent-aided UWB breast imaging," *IEEE Trans. Biomed. Eng.*, Vol. 57, No. 5, 1003–1007, 2010.
7. Chen, Y. and P. Kosmas, "Detection and localization of tissue malignancy using contrast-enhanced microwave imaging: Exploring information theoretic criteria," *IEEE Trans. Biomed. Eng.*, Vol. 59, No. 3, 766–776, Mar. 2012.
8. Santorelli, A., E. Porter, E. Kirshin, Y. J. Liu, and M. Popovic, "Investigation of classifiers for tumor detection with an experimental time-domain breast screening system," *Progress In Electromagnetics Research*, Vol. 144, 45–57, 2014.
9. Conceicao, R. C., H. Medeiros, M. O'Halloran, D. Rodriguez-Herrera, D. Flores-Tapia, and S. Pistorius, "SVM-based classification of breast tumour phantoms using a UWB radar prototype system," *2014 XXXIth URSI General Assembly and Scientific Symposium (URSI GASS)*, 1–4, 2014.
10. Zastrow, E., S. K. Davis, M. Lazebnik, F. Kelcz, B. D. Van Veen, and S. C. Hagness, "Database of 3D grid-based numerical breast phantoms for use in computational electromagnetics simulations," Online Available: http://uwcem.ece.wisc.edu/MRIdatabase/.
11. Lazebnik, M., M. Okoniewski, J. H. Booske, and S. C. Hagness, "Highly accurate debye models for normal and malignant breast tissue dielectric properties at microwave frequencies," *IEEE Microw. Wirel. Compon. Lett.*, Vol. 17, No. 12, 822–824, 2007.
12. Oliveira, B., M. Glavin, E. Jones, M. O'Halloran, and R. Conceicao, "Avoiding unnecessary breast biopsies: Clinically-informed 3D breast tumour models for microwave imaging applications," *2014 IEEE APSURSI*, 1143–1144, 2014.
13. Shahzad, A., M. O'Halloran, M. Glavin, and E. Jones, "A novel optimized parallelization strategy to accelerate microwave tomography for breast cancer screening," *2014 36th Annual International Conference of the IEEE Engineering in Medicine and Biology Society (EMBC)*, 2456–2459, 2014.
14. Shlens, J., "A tutorial on principal component analysis," ArXiv Prepr. ArXiv14041100, 2014.
15. Hsu, C. W., C. C. Chang, and C. J. Lin, "A practical guide to support vector classification," 1–16, SeerX, 2003.